Defence Science Journal, Vol. 63, No. 4, July 2013, pp. 435-441, DOI: 10.14429/dsj.63.4870

Preparation, Characterisation and Photocatalytic Applications of TiO_2-MWCNTs Composite

Kirti D. Shitole, Roshan K. Nainani, and Pragati Thakur*

University of Pune, Pune-411 007, India
**E-mail:prthakur@chem.unipune.ac.in*

ABSTRACT

The nanocomposite of *TiO_2-MWCNTs* has been synthesised by simple hydrothermal route showing significant enhancement in the photocatalytic activity for the degradation of methyl orange dye (MO). Several characterisations employed were X-ray diffraction (XRD), Scanning electron microscopy (SEM), Energy-dispersive X-ray spectroscopy (EDX), Transmission electron microscopy (TEM), Raman spectroscopy.XRD pattern shows the formation of anatase phase in prepared *TiO_2* which was retained in *TiO_2-MWCNTs* composite as well. The Raman spectrum of prepared *TiO_2-MWCNT* shows the interface integration of *TiO_2* and *MWCNTs* which is further supported by TEM data. Complete decolorisation and degradation of dye using *TiO_2-MWCNTs* nanocomposite has been observed only in 45 minutes of UV irradiation. 65 per cent reduction in chemical oxygen demand (COD) value of treated dye shows substantial mineralisation of dye by composite catalyst. Dye degradation reactions were found to follow first order kinetics.

Keywords: *MWCNTs, TiO_2,* methyl orange, photocatalysis

1. INTRODUCTION

Titanium dioxide is a benchmark photocatalyst for the successful decontamination of the organic pollutants in both liquid and gas phases. Although *TiO_2* has several advantages, it has two critical limitations for large scale technical applications. They are (i) electron hole recombination which limits its efficiency[1]. (ii) it absorbs only 2-3% of the solar light impinging on the earth's surface as it can be excited only under UV irradiation with wavelengths shorter than 400 nm. To overcome the limitations innumerable methods have been applied to enhance the photocatalytic activity of *TiO_2* by increasing active sites of reaction, retardation of electron–hole recombination and visible light catalysis by modification of band–gap[2-4]. Recently, among carbon materials, after the discovery of carbon nanotubes[5], *TiO_2-MWCNTs* composites have attracted much attention of researchers because of the remarkable electrical[6-7], mechanical[8] and thermal[9] properties of *MWCNTs* and the promising applications of *TiO_2-MWCNTs* composites for the big problem of pollutions[10] due to their high capability to conduct electrons and adsorb hydrophobic organic pollutants, hardly adsorbed by *TiO_2* nanoparticles themselves[11,12]. The synergistic effect of carbon nanotubes on the activity of composite catalyst can be explained in terms of its action as adsorbent and dispersing agent. Further *MWCNTs* consisting of multiple layers of graphite superimposed and rolled in on them to form tubular shape conductive structure might facilitate the separation of the photo-generated electron/hole pairs at the *TiO_2-CNT* interface leading to the faster rates of photocatalytic oxidation and enhancement in the efficiency of titanium dioxide.

Different techniques have been employed for the preparation of *TiO_2-CNTs* composites. Mostly *TiO_2* is coated on the surface of CNT. The composites can be prepared by various methods[13,14] which includes sol-gel,[15-18] impregnation[19], electro-spinning,[20,21] electrophoretic deposition[22], chemical vapor deposition[23] and hydrothermal method[24]. Among this sol-gel has been used extensively for mechanical mixing of *CNT-TiO_2* composites[25,26]. Composites prepared by hydrothermal methods are mostly found to give better results as it favors a decrease in agglomeration among particles, narrow particle size distribution, phase homogeneity and controlled particle morphology. In the present study, we have prepared *TiO_2-MWCNTs* nanocomposites by in-situ deposition of *TiO_2* on the *MWCNTs* by hydrothermal treatment.

2. EXPERIMENTAL

2.1 MWCNTs Functionalization

The pristine *MWCNTs* (Multi Walled Carbon Nanotubes) were purchased from Plasma Chem. GmbH Berlin, having diameters of 5-20 nm, lengths of 1-10 μm and carbon purity is minimum 95%**.** Purification and functionalisation of *MWCNTs* is needed to remove impurities and to improve the solubility of *MWCNTs* in water by introducing anionic groups on their surfaces[27].

In a typical purification treatment, 1g pristine *MWCNTs* were sonicated in the equal volume of conc. HCl for 1 hr and allowed to settle down, after settling yellow coloured supernatant acid was observed. This colour indicates that there is a *Fe* impurity present in the pristine *MWCNTs*. This *Fe* impurity has been removed by repeating same procedure

Received 22 March 2013, revised 10 June 2013, online published 19 July 2013

and removing the acid layer on the surface of *MWCNTs* till the supernatant acid became colorless. The clear supernatant acid confirms the complete removal of iron impurity. These purified *MWCNTs* were further washed with doubled distilled water till complete removal of acid was achieved, which was confirmed by litmus paper and then dried at 110 °C in hot air oven for about 6-7 hrs[28]. For functionalization, purified *MWCNTs* were refluxed in conc. HNO_3 for 6 hrs at boiling temperature of acid (≈80°C). After refluxing the above solution, it was allowed to cool to room temperature and decanted the upper layer of acid. It was then washed several times with double distilled water till neutral pH was achieved, which was confirmed by performing litmus paper test and was then dried at 110 °C in vacuum oven for 6-7 hrs. The dried MWCNTs were collected and subjected for FTIR analysis[27].

2.2 Synthesis of TiO_2 and TiO_2-MWCNTs Nanocomposite

Titanium dioxide and *TiO_2-MWCNTs* nanocomposite were prepared by hydrothermal method, using titanium tetraisopropoxide (TTIP) as the precursor[29]. For synthesis all used chemicals were of analytical grade. In synthesis of *TiO_2-MWCNTs* nanocomposite, the functionalized *MWCNTs (fMWCNTs)* were added to provide a weight ratio of *MWCNTs* over TiO_2 as 10%. First *fMWCNTs* were dispersed into double distilled water and sonicated for 1h. A predetermined amount of TTIP was mixed with ethanol in 1:5 ratios. After complete dispersion of *MWCNTs* in water, TTIP. Ethanol solution was added drop wise under sonication and was kept overnight with vigorous stirring. On the next day, whole solution was transferred to the Teflon lined stainless steel autoclave and was placed in muffle furnace for hydrothermal treatment at 140 °C for 24h. In autoclave *fMWCNTs* interact with *TiO_2* at high temperature and at elevated pressure. After cooling the furnace to the room temperature autoclave was removed from the furnace opened and dried the composite formed on hot plate. The composite was calcined at 400 °C for 2h. The photocatalytic efficiency of the composite was compared with bare Titanium dioxide prepared by same method without adding *fMWCNTs*.

2.3 Characterisation of Sample

The *TiO_2* and *TiO_2-MWCNTs* nanocomposite were characterized by a range of analytical techniques. The X-ray powder diffraction (Philips X' Pert PRO) patterns were recorded with *Cu Kα* radiation (α = 0.15406 nm) in the range 10° to 80° 2θ at a scanning speed of 0.02° s^{-1} to determine the crystal structure. The Raman measurements were performed by Micro Raman Spectroscopy (Horiba Jobin Yvon Lab RAM HR 800 spectrometer) for the study of chemical bonding and nature of disorder in the materials. The morphology and structure of *TiO_2* nanoparticle and *TiO_2-MWCNTs* nanocomposite were examined by Transmission electron microscopy (*TECNAI G^2* 20 TWIN FEI, Netherlands) and Scanning electron microscopy (JEOL JSM-6360 A) along with Energy Dispersive X-ray (EDX). The sample was subjected to thermal gravimetric analysis (DTG-60H simultaneous DTA-TG apparatus, Shimadzu) to get information regarding thermal stability of the composite. The formation of functional groups on the surface of pristine *MWCNTs* after acid treatment was studied by the FTIR spectroscopy (Shimadzu FTIR-8400 spectrophotometer) with KBr-disc technique.

2.4 Photocatalytic Activity

The photocatalytic activities of the *TiO_2* nanoparticles and *TiO_2-MWCNTs* nanocomposite were monitored from the results of photocatalytic degradation of methyl orange. The initial concentration of methyl orange was 0.01mmols and catalyst dose was 0.02g/50 mL. The reaction temperature was controlled at 30±1°C by an air cooling. The photocatalytic activity was analysed using homemade multilamp photoreactor consisting of quartz reaction vessel in the center surrounded by four 8W UV lamps at the edges of the square. The reaction solution was constantly aerated using aerator pump (Philips, TUV 8W/G8 T5). Before UV irradiation the suspension was stirred in dark for 1h to ensure the establishment of adsorption-desorption equilibrium. The concentration of un-decomposed methyl orange at various time intervals during UV irradiation was determined using Shimadzu UV-visible (UV-1800 PC) spectrophotometer. Conversion of methyl orange was defined as the following :

$$\% \text{ conversion} = (C_0 - C)/C_0 \times 100$$

where C_0 is the initial concentration of methyl orange and C is the concentration of methyl orange after photocatalytic reaction[16]. The photocatalytic degradation and mineralisation of methyl orange was further confirmed by COD analysis. For COD, the digestion of sample was carried out by open reflux method using COD digester (Spectralab COD digestor 2015M) for 2h at 150 °C. After cooling, the solutions were titrated against ferrous ammonium sulfate by COD titrator (Spectralab COD titrator CT-15) using double distilled water as a blank solution.

3. RESULTS AND DISCUSSIONS

3.1 Crystal Structure

The XRD of *TiO_2* (refer Fig.1 c) shows the formation of anatase and brookite mixture. The peaks for anatase are 25.33(101), 37.88(004), 47.98(200), 54.74(105), 62.80(204), 70.00(116), 75.16(301) [JCPDS 21-1272] and one small peak for brookite 30.68(211) [JCPDS 76-1 937]. XRD of MWCNTs (Fig 1(a)) shows two characteristic peaks at 26.00(002) and

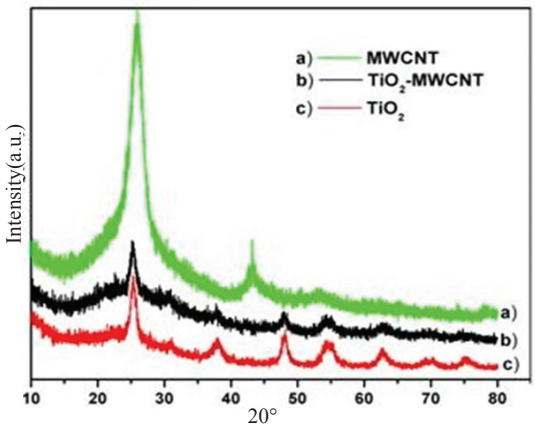

Figure 1. XRD patterns of (a) *MWCNTs* (b) *TiO_2-MWCNTs* (c) *TiO_2*.

43.11(100) [JCPDS 41-1487]. The composite shows all these above mentioned peaks confirming the formation of *TiO_2-MWCNTs* nanocomposite (Fig. 1(b)).

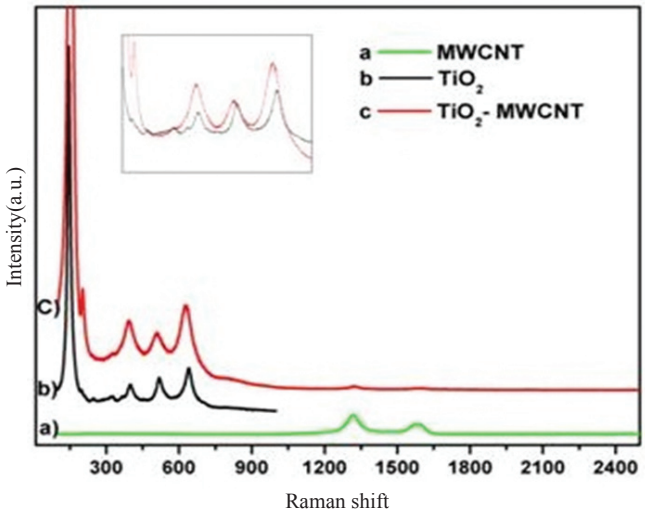

Figure 2. Raman spectrum of (a) *MWCNTs* (b) *TiO_2*(c) *TiO_2-MWCNTs.*

The Raman spectra for *TiO_2*, *MWCNTs* and *TiO_2-MWCNTs* nanocomposite samples are as shown in Fig. 2. The Raman spectrum for the pure *TiO_2* assign the 148.10 cm^{-1} (very strong Eg), 397.82 cm^{-1} *(B_{1g})*, 518.07 cm^{-1} *(A_{1g})* and 641.53 cm^{-1} *(E_g)* bands to anatase[30-31] and 246.89 cm^{-1} *(A_{1g})* and 326.17 cm^{-1} *(B_{1g})* bands to brookite[32]. It confirms the preparation of *TiO_2* as a mixture of anatase and brookite, anatase phase being dominant, which was earlier confirmed by XRD data. In the Raman spectrum of *MWCNTs* the band at 1597.21 cm^{-1} indicates the G band, this G band shows the crystalline nature of the *MWCNTs*. The band at 1318 cm^{-1} (D band) indicates the distortions on the *MWCNTs* surface. It is worth noting that the synergistic effect occurs only if the *TiO_2* is chemically attached to the carbon nanotubes[33]. The main three bands (397.82 cm^{-1}, 518.07 cm^{-1}, 641.53 cm^{-1}) in the Raman spectrum representative of anatase *TiO_2* (refer Fig. 2 : inset) are broadened and shifted in the case of *TiO_2-MWCNTs* nanocomposite sample as compared to the pure *TiO_2*. Such broadening and shifting may occur due to strain gradients originating from interface integration of *TiO_2* and *MWCNT*[34].

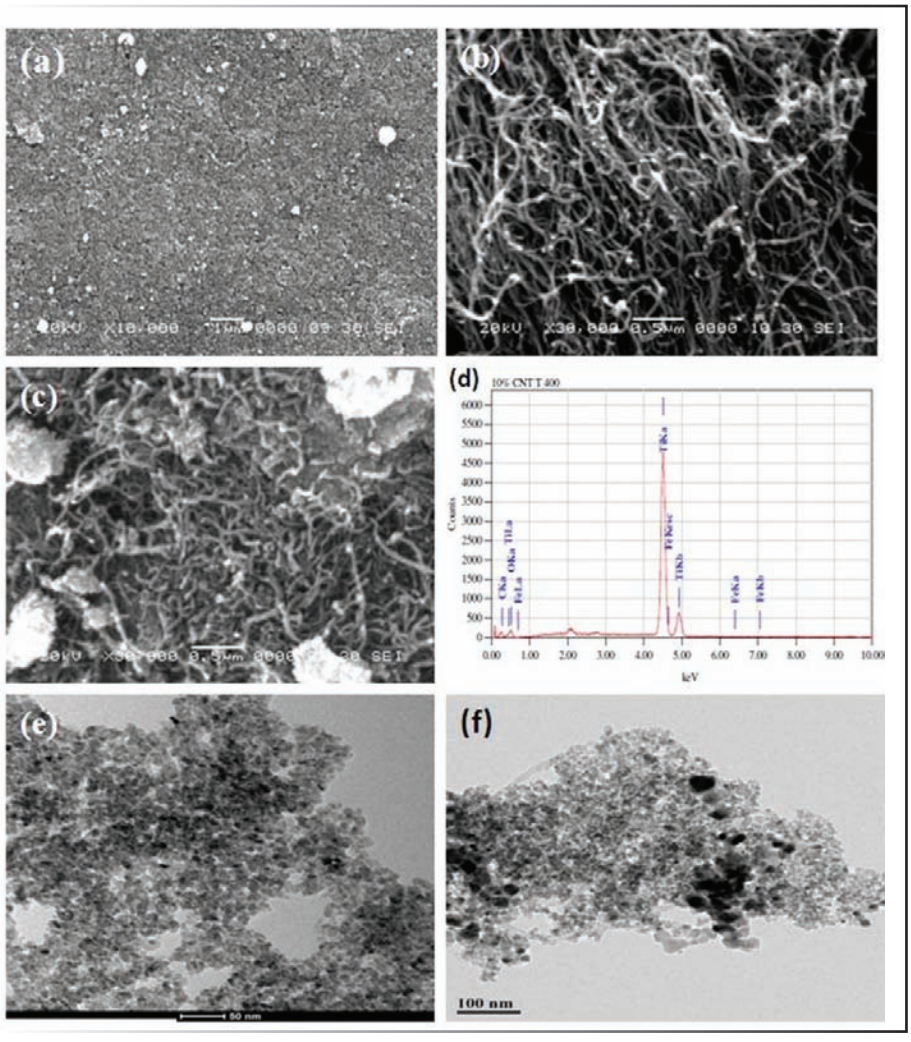

Figure 3. SEM images of the (a) synthesised *TiO_2* (b) *MWCNTs* (c) *TiO_2-MWCNTs* nanocomposite (d) EDX of the *TiO_2-MWCNTs* nanocomposite and TEM images of the (e) synthesized *TiO_2* (f) *TiO_2-MWCNTs* nanocomposite.

3.2 Morphological Characterisation

Figures 3(a), 3(b) and 3(c) shows the SEM images of TiO_2, *MWCNTs* and TiO_2-*MWCNTs* nanocomposite. The TEM images of TiO_2 and TiO_2-*MWCNTs* nanocomposite are shown in Figs. 3(e) and 3(f). SEM and TEM images of TiO_2 shows the uniform average distribution. Figure 3(c) depicts the SEM of TiO_2-*MWCNTs* nanocomposite showing TiO_2 nanoparticles agglomeration on *MWCNTs* surface. The TEM image (Fig. 3(f)) reveals nanocomposite formation made up of TiO_2 nanoparticle agglomerates embedded with *MWCNTs*[35]. Because of the more quantity of TiO_2 over *MWCNTs* (10% *MWCNTs* content) most of the *MWCNTs* are covered and hidden under the TiO_2 nanoparticles. The aggregation of TiO_2 over *MWCNTs* indicates the supporting role of *MWCNTs* as center for deposition and growth of TiO_2 nanoparticles[35]. Also confirming the intimate contact between the *MWCNTs* and TiO_2. The energy dispersive X-ray (Fig. 3(d)) spectrum analysis of TiO_2-*MWCNTs* samples shows the presence of *C, O* and Ti elements.

3.3 Thermogravimetric Analysis

The TGA gives information about thermal stability of compound. As seen in Fig. 4, the highest rate of mass loss is at 500 °C which is the combustion point of *MWCNTs*. In case of TGA of TiO_2, initial loss in weight can be seen due to evaporation of water molecules around 100 °C and further due to decomposition of organic residue around 200 °C - 350 °C. In the composite of TiO_2-*MWCNTs*, the early weight loss around 100 °C was because of water evaporation followed by decomposition of organic residue and combustion of *MWCNTs* around 200-350 °C and 550-650 °C respectively[36]. The thermal analysis suggests the stability of TiO_2- *MWCNTs* nanocomposite at calcination temperature of 400 °C. Further the *MWCNTs* present in composite are thermally more stable than pristine *MWCNTs*.

3.4 FTIR Spectroscopy

To obtain the hydrophilic surface structure of oxygen containing surface groups, chemical oxidation of *MWCNTs* is carried out using concentrated nitric acid. The oxidation of *MWCNTs* with nitric acid introduces some functional groups like-*OH (Hydroxyl)*,-*COOH (carboxyl)* and some more on the surface of *MWCNTs*[16]. These surface groups are helpful to form interaction and chemical bonding between *MWCNTs* and TiO_2. The FTIR spectrum of pristine (refer Fig.5(a)) and functionalised *MWCNTs* provides information of surface functional groups. As shown in Fig. 5(b) functionalised *MWCNTs* exhibits characteristic strong and broad band between 3173-3600 cm^{-1} which can be attributed to *O-H* stretching vibrations in *C-OH* groups. The broad band between 1766-2017 cm^{-1} is attributed to *C=O* stretching vibrations in carboxyl, aldehyde and acid anhydride groups[37].

3.5 Photocatalytic Application

The photocatalytic activity of TiO_2 and TiO_2-*MWCNTs* was evaluated by studying the oxidation of methyl orange dye solution under UV light irradiation. Figures 6(a) and 6(b) shows UV-Visible absorbance spectral changes of methyl orange dye solution during the photocatalytic degradation in the presence of prepared TiO_2 and prepared TiO_2-*MWCNTs* nanocomposite. Obtained results show (refer Fig. 6(c)), two fold enhancement in the photocatalytic activity of TiO_2-*MWCNTs* nanocomposite as compared to pure prepared TiO_2 nanoparticles in only 45 minutes of UV irradiation**.** Degradation of methyl orange dye

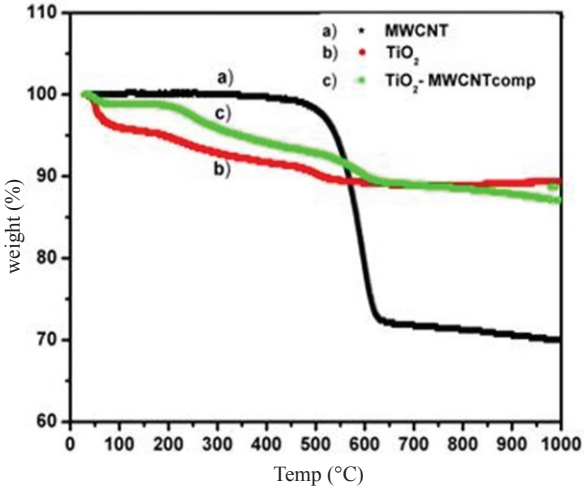

Figure 4. TGA graph of the (a) *MWCNTs* (b) TiO_2-*MWCNTs* (c) TiO_2.

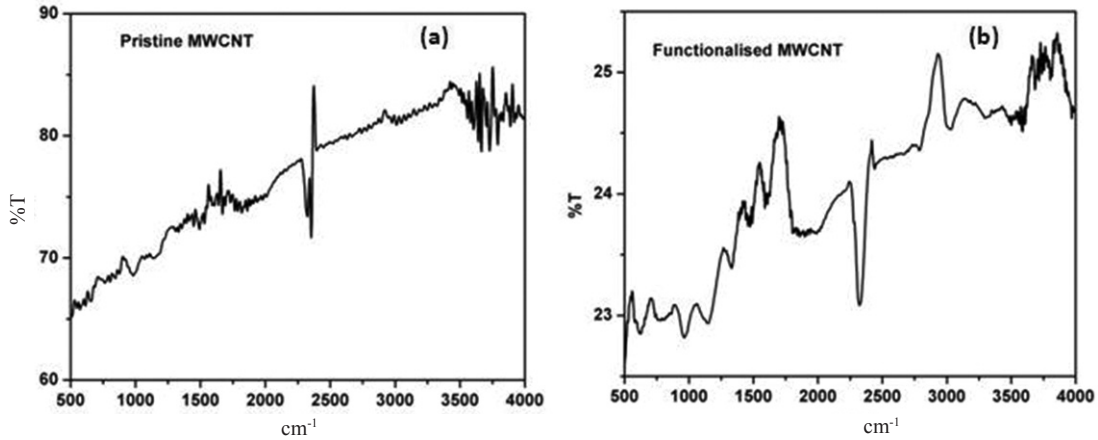

Figure 5. FTIR spectrum of (a) Pristine *MWCNTs* (b) functionalized *MWCNTs*.

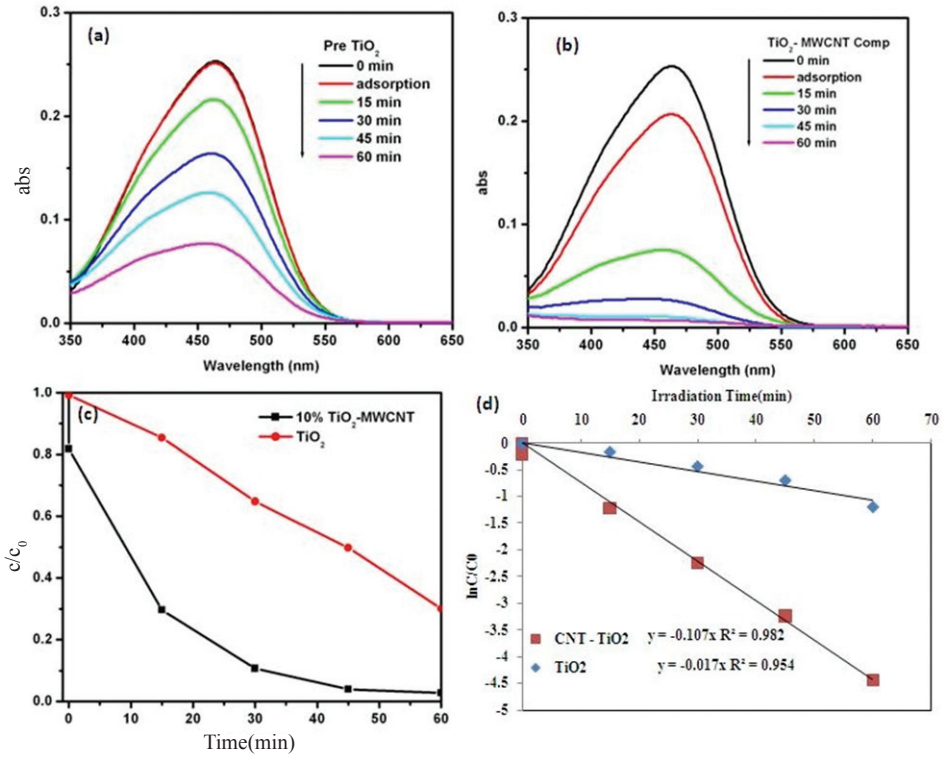

Figure 6. Absorption spectra for the photo catalytic degradation of MO using catalyst (a) *TiO*$_2$ (b) *TiO*$_2$*-MWCNTs* nanocomposite (c) *C/C0* vs time for photodegradation of methy1orange dye solution (d) kinetics of photodegradation of MO by prepared *TiO*$_2$ and *TiO*$_2$*-MWCNTs* nanocomposite concentration of Mo=0.01mmols, catalyst dose=0.02g/50ml.

was found to follow the first order reaction kinetics (refer Fig. 6d). The obtained results show that the rate of degradation of Methyl Orange dye using *TiO*$_2$*-MWCNTs* nanocomposites as photocatalyst is 10 times higher as compared to prepared *TiO*$_2$. The enhanced photocatalytic efficiency of as synthesized nanocomposite can be attributed to the presence of *MWCNTs* which act as an adsorbent, dispersing agent and electron reservoir facilitating the separation of the photo-generated electron-hole pairs at the *TiO*$_2$*-MWCNTs* interface leading to the faster rates of photocatalytic oxidation[19].

The COD data depicted in Table 1 shows substantial degradation and mineralisation of methyl orange dye solution when *TiO*$_2$*-MWCNTs* nanocomposite was used.

Table 1. The percentage reduction in COD

S No.	Photocatalyst	Per cent reduction of COD
1	TiO_2-MWCNT	64.00
2	TiO_2	46.23
3	Without catalyst	12.05

4. CONCLUSION

Nanosized and interface integrated *TiO*$_2$*-MWCNTs* composite was successfully synthesised using hydrothermal method and was further characterized by XRD, Raman spectroscopy, SEM, TEM, EDX, FTIR and TGA techniques. The enhanced photocatalytic efficiency of as synthesised *TiO*$_2$*-MWCNTs* nanocomposite suggests that the *MWCNTs* acts as an adsorbent, dispersing agent and electron reservoir and hence facilitating the separation of the photo-generated electron-hole pairs at the *TiO*$_2$*-MWCNT* interface leading to the faster rates of photocatalytic oxidation. Degradation of methyl orange dye was found to follow the first order reaction kinetics. COD values of degraded methyl orange dye solution shows substantial mineralisation when *TiO*$_2$*-MWCNTs* nanocomposite was used.

ACKNOWLEDGEMENTS

Authors are thankful to ISRO-UoP Cell, Pune University for research funding. Authors would like to acknowledge Dr. Suresh Gokhale, NCL, Pune for Raman characterisation and Prof. Santosh Haram, Department of Chemistry, University of Pune for fruitful discussion.

REFERENCES

1. Byrappa, K.; Dayananda, A.S.; Sajan, C.P.; Basavalinga, B.; Shayan, M.B.; Soga, K. & Yoshimura, M. Hydrothermal preparation of *ZnO:CNT* and *TiO*$_2$*:CNT* composites and their photocatalytic application. *J. Mater. Sci.*, 2008, **43(7)**, 2348-2355.
2. Kubacka, A.; Fernandez, M. & Colon, G. Advanced nanoarchitectures for solar photocatalytic applications. *Chem. Rev.*, 2012, **112**(3), 1555-1614.
3. Nainani, R.; Chaskar, M. & Thakur, P. Synthesis of silver doped *TiO*$_2$ nanoparticles for the improved photocatalytic degradation of methyl orange. *J. Mater. Sci. and Eng. B*, 2012, **2**(1), 52-58.
4. Mauter, M.S. & Elimelech, M.E. Environmental

applications of carbon-based nanomaterials. *Environ. Sci. Technol.,* 2008, **42**(16), 5843-5859.

5. Ijima, S. Helical microtubules of graphitic carbon, *Nature,* 1991, **354**, 56-58.
6. Krishna, A.; Duradin, E.; Ebbesen, T.W.; Yilanilos, P.N. & Treacy, M. Young's modulus of single-walled nanotubes, *Phys. Rev. B,* 1998, **58** (20), 14013-14021.
7. Wong, E.; Sheehan, P. & Liber, C. Nanobeam mechanics: elasticity, strength, and toughness of nanorods and nanotubes. *Science*, 1997, 277(5334) 1971-75.
8. Sandler, J.; Kirk, J.; Kinloch, I.; Shaffer, M. & Windle, A. Ultra-low electrical percolation threshold in carbon-nanotube-epoxy composites. *Polymer,* 2003, **44**(19), 5893-5901.
9. Hone, J.; Laguno, M.; Biercuk, M.; Johnson, A.; Batlogg, B.; Benes, Z. & Fischer, Thermal properties of carbon nanotubes and nanotube-based materials. *J. App. Phys. A,* 2002, **74**(3), 339-335.
10. Schnorr, J.M. & Swager, T.M. Emerging applications of carbon nanotubes. *Chem. Mater.,* 2011, **23**(3), 646-657.
11. Tasis, D.; Tagmatarchis, N.; Bianco, A. & Prato, M. Chemistry of carbon nanotubes. *Chem. Rev.,* 2006,**106**(3), 1105-1136.
12. Eder, D. Carbon nanotube-inorganic hybrids. *Chem. Rev.,* 2010, **110**(3), 1348-1385.
13. Woan, K.; Pyrgiotakis, G. & Sigmund, W. Photocatalytic carbon-nanotube–TiO_2 composites. *Adv. Mater.,* 2009, **21**(21), 2233-2239.
14. Leary, R.; Westwood, A. Carbonaceous nanomaterials for the enhancement of TiO_2 photocatalysis. *Carbon,* 2011,**49**(3), 741-772.
15. Bouazza, N.; Ouzzine, M.; Lillo-Rodenas, M.A.; Eder, D. & Linares-Solano, A. TiO_2 nanotubes and *CNT-*TiO_2 hybrid materials for the photocatalytic oxidation of propene at low concentration. *Appl. Catal. B: Environ.,* 2009 , **92**(3-4), 377-383.
16. Yan, X.; Kang, T.B. & Yang, Y. Dispersing and functionalising multiwalled carbon nanotubes in TiO_2 sol. *J. Phys. Chem. B,* 2006, **110**(51), 25844-25849.
17. Zhang, K.; Zhang, F.J.; Chen, L.M. & Oh, W.C. Comparison of catalytic activities for photocatalytic and sonocatalytic degradation of methylene blue in present of anatase TiO_2*–CNT* catalysts. *Ultrason. Sonochem.,* 2011,**18**(3), 765-772.
18. Wang, W.; Serp, P.; Kalck, P. & Faria, L.J. Visible light photodegradation of phenol on MWNT-TiO_2 composite catalysts prepared by a modified sol-gel method. *J. Mol. Catal. A: Chem.,* 2005, **235**(1-2), 194-199.
19. Xu, Y.; Zhuang, Y. & Fu, X. New insight for enhanced photocatalytic activity of TiO_2 by doping Carbon nanotubes: A case study on degradation of benzene and methyl orange. *J. Phys. Chem.,* 2010, **114**(6), 2669-76.
20. Hu, G.; Meng, X. & Feng, X.; Anatase TiO_2 nanoparticles/ carbon nanotubes nanofibers: preparation, characterisation and photocatalytic properties. *J. Mater. Sci.,* 2007, **42**, 7161-7170.
21. Aryal, S.; Kim, C.K. & Kim, K.W. Multi-walled carbon nanotubes/TiO_2 composite nanofiber by electrospinning. *Mater. Sci. Eng. C,* 2008, **28**(1), 75-79.
22. Cho, J.; Schaab, S. & Roether, J.A. Nanostructured carbon nanotube/TiO_2 composite coatings using electrophoretic deposition (EPD). *J. Nanopart. Res.,* 2008, **10**(1), 99-105.
23. Yu, H.; Quan, X. & Chen, S. TiO_2-multiwalled carbon nanotube heterojunction arrays and their charge separation capability. *J. Phys. Chem. C,* 2007, **111**(35), 12987-91.
24. Chen, H.; Yang, S.; Yu, K.; Ju ,Y. & Sun, C. Effective photocatalytic degradation of atrazine over titania-coated carbon nanotubes (CNTs) coupled with microwave energy. *J. Phys. Chem.,* 2011,**115**(14), 3034-3041.
25. Ming-liang, C.; Feng-jun, Z. & Oh, W. Synthesis, characterisation, and photocatalytic analysis of *CNT/* TiO_2 composites derived from *MWCNTs* and titanium sources. *New Carbon Mater.,* 2009, **24**(2), 159-166.
26. Yu, J.; Fan, J. & Cheng, B. Dye-sensitised solar cells based on anatase TiO_2 hollow spheres/carbon nanotube composite films. *J. Power Sources,* 2011,**196**(18), 7891-7898.
27. Moon, J.M.; An, K. & Lee, Y. H. High-yield purification process of singlewalled carbon nanotubes. *J. Phys. Chem. B,* 2001, **105**(24), 5677-5681
28. Samant, K.M.; Chaudhari, V.R.; Kapoor, S. & Haram, S.K. Filling and coating of multi -walled carbon nanotubes with silver by DC electrophoresis. *Carbon*, 2007, **45**(10), 2126.
29. Thakur, P. & Nainani, R. Synthesis of sol-gel derived TiO_2 nanoparticles for the photocatalytic degradation of methyl orange dye. *Res. J. Chem. Environ.,* 2011,**15**(2), 145-149.
30. Gotic, M.; Ivanda, M.; Popovic, S.; Music, S.; Sekulic, A.; Turkovic, A. & Furic, K. Raman investigation of nanosized TiO_2. *J. Raman Spectrosc.,* 1997, **28**(7), 555-558.
31. Dlamini, L.N.; Krause, R.W.; Kulkani, G.U. & Durbach, S.H. Photodegradation of bromophenol blue with fluorinated TiO_2 composite. *Appl. water sci*., 2011,**1**(1-2), 19-24.
32. Tompsett, G.A.; Bowmaker, G.A.; Cooney, R.P.; Metson, J. B.; Rodgers, K.A. & Seakins, J.M. The Raman spectrum of brookite, TiO_2 *(Pbca, Z = 8). J. Raman Spectrosc.,*1995, **26**(1), 57-62.
33. Inoue, F.; Ando, R. A. & Corio, P. Raman evidence of the interaction between multi-walled carbon nanotubes and nanostructured TiO_2. *J. Raman Spectrosc.,* 2011, **42**(6), 1379-1383.
34. Muduli, S.; Lee, W.; Dhas, V.; Mujawar, S.; Dubey, M.; Vijayamohanan, K.; Han, S. & Ogale, S. Enhanced conversion efficiency in dye-sensitized solar cells based on hydrothermally synthesised TiO_2*-MWCNT* nanocomposites. *Appl. Mater.Interfac*., 2009, **1**(9), 2030-35.
35. Gao, B.; Chen, G.Z. & Puma, G.L. Carbon nanotubes/ titanium dioxide *(CNTs/*TiO_2*)* nanocomposites prepared by conventional and novel surfactant wrapping sol-gel methods exhibiting enhanced photocatalytic activity. *Appl. Catal. B: Environ.,* 2009, **89**(3-4), 503-509.
36. Li, Z.; Gao, B.; Chen, G.Z.; Mokaya, R.; Sotiropoulos, S. & Puma, G.L Carbon nanotubes/titanium dioxide *(CNTs/*TiO_2*)* core shell nanocomposites with tailored

shell thickness, CNT content and photocatalytic/ photoelectrocatalytic properties.*Appl. Catal. B: Environ.,* 2011, **110** (issue no.), 50-57.

37. Kovtyukhova, N.I.; Mallouk, T.E.; Pan, L. & Dickey, E.C. Individual single-walled nanotubes and hydrogels made by Oxidative Exfoliation of carbon nanotube ropes. *J. Am. Chem. Soc.,* 2003, **125**(32), 9761-9769.

Contributors

Ms Kirti D. Shitole received her MSc in Analytical Chemistry in 2009 from Department of Chemistry, Pune University, India and currently pursuing her MPhil in Material Chemistry from the same University. Her research work involves synthesis, characterisation and photocatalytic applications of nanocomposites of metal oxides.

Mr Roshan K. Nainani has done MSc (Physical Chemistry) from Mumbai University and MPhil in Physical Chemistry from Department of Chemistry, Pune University, India. Presently, he is pursuing PhD in Physical Chemistry at Department of Chemistry, Pune University. His research interests are synthesis of metal oxide nanoparticles and their nanocomposite with graphene oxide and zeolites for applications in photocatalytic degradation of hazardous pollutants, photocatalytic hydrogen evolution etc.

Dr Pragati Thakur received her PhD from Laxminarayan Institute of Technology, Nagpur University in 2003. After that, she joined as a Lecturer in Physical Chemistry at Department of Chemistry, Pune University, Pune. Presently, she is working as an Associate Professor of Physical Chemistry in Pune University. Her areas of research include: Synthesis of semiconductor nanoparticles and their composites with carbon nanotubes, graphene oxide etc. for applications in energy and environment, heterogeneous photocatalysis, photocatalytic water splitting, industrial wastewater treatment, solar cells etc.